THE JOURNAL OF BIOLOGICAL CHEMISTRY
Vol. 279, No. 47, Issue of November 19, pp. 49222–49228, 2004
Printed in U.S.A.

Amino Acids of the *Sulfolobus solfataricus* Mini-chromosome Maintenance-like DNA Helicase Involved in DNA Binding/Remodeling*

Received for publication, August 5, 2004
Published, JBC Papers in Press, September 14, 2004, DOI 10.1074/jbc.M408967200

Biagio Pucci‡, Mariarita De Felice‡, Mosè Rossi‡, Silvia Onesti§, and Francesca M. Pisani‡¶

From the ‡Istituto di Biochimica delle Proteine, Consiglio Nazionale delle Ricerche, Via P. Castellino 111, 80131 Napoli, Italy and the §Department of Biological Sciences, Imperial College, London SW7 2AZ, United Kingdom

Herein we report the identification of amino acids of the *Sulfolobus solfataricus* mini-chromosome maintenance (MCM)-like DNA helicase (SsoMCM), which are critical for DNA binding/remodeling. The crystallographic structure of the N-terminal portion (residues 2–286) of the *Methanothermobacter thermoautotrophicum* MCM protein revealed a dodecameric assembly with two hexameric rings in a head-to-head configuration and a positively charged central channel proposed to encircle DNA molecules. A structure-guided alignment of the *M. thermoautotrophicum* and *S. solfataricus* MCM sequences identified positively charged amino acids in SsoMCM that could point to the center of the channel. These residues (Lys-129, Lys-134, His-146, and Lys-194) were changed to alanine. The purified mutant proteins were all found to form homo-hexamers in solution and to retain full ATPase activity. K129A, H146A, and K194A SsoMCMs are unable to bind DNA either in single- or double-stranded form in band shift assays and do not display helicase activity. In contrast, the substitution of lysine 134 to alanine affects only binding to duplex DNA molecules, whereas it has no effect on binding to single-stranded DNA and on the DNA unwinding activity. These results have important implications for the understanding of the molecular mechanism of the MCM DNA helicase action.

The eukaryotic mini-chromosome maintenance (MCM)[1] complex consists of six paralog proteins (MCM2–7; for a review see Refs. 1 and 2) that belong to the AAA$^+$ (ATPases with other associated cellular activities) superfamily (3). The *Saccharomyces cerevisiae* MCM genes were all shown to be essential in both the initiation and elongation phases of DNA replication (4). MCM genes were also identified in other eukaryotic organisms (such as *Schizosaccharomyces pombe*, *Drosophila melanogaster*, *Xenopus laevis*, and *Homo sapiens*), and in several cases the corresponding protein products were purified from cell extracts of the above species as complexes of variable subunit composition (such as MCM2/3/4/5/6/7, MCM2/4/6/7, MCM4/6/7, and MCM3/5) (5–7). Among all of these multimeric assemblies, a hexamer comprising the subunits MCM4, MCM6, and MCM7 of *H. sapiens* (8), *Mus musculus* (6), and *S. pombe* (7, 9) displayed a weak DNA helicase activity *in vitro*, whereas MCM2 and MCM3/5 caused the disassembly of the pre-formed MCM4/6/7 hexamers and inhibited the helicase activity (6–8, 10–11). This led to the suggestion that the complex is formed by three active subunits (MCM4, MCM6, and MCM7) and three subunits with a regulatory role (MCM2, MCM3, and MCM5). However, site-directed mutagenesis studies indicated that physical association between specific proteins of the two groups is required for efficient ATPase activity (12–13).

Despite a number of studies suggesting that in eukaryotic organisms the MCM complex could act as the replicative DNA helicase, some concern was caused by the limited processivity of its DNA unwinding activity *in vitro*. The most direct piece of evidence that the MCM complex possesses DNA helicase activity comes from studies of the homolog proteins of Archaea. Whereas eukaryotes possess six paralogs, most archaeal species examined contain a single MCM homologue (14–15). To date, the MCM-like complex has been characterized only from three archaeal organisms, namely *Methanothermobacter* (previously named *Methanobacterium*) *thermoautotrophicum* (MthMCM) (16–21), *Sulfolobus solfataricus* (SsoMCM) (22), and *Archaeoglobus fulgidus* (AfuMCM) (23). These studies revealed that the archaeal enzymes possess a robust and processive 3′ to 5′ helicase activity, a single- and double-stranded DNA binding function, and ATPase activity. Lee and Hurwitz reported that the *S. pombe* MCM4/6/7 complex is significantly stimulated on forked DNA structures and can unwind duplex molecules up to ~600 base pairs on 5′-tailed substrates (9).

The oligomeric structure of the archaeal MCM complex is still not clear. Whereas the MthMCM produced in *Escherichia coli* was reported to form dodecamers (16–19), the recombinant SsoMCM (22) and *A. fulgidus* MCM (23) were both shown to behave as homo-hexamers in solutions. Electron microscopy analyses of MthMCM revealed ring-shaped hexameric (24) or heptameric (25) assemblies. A toroidal hexameric structure was also observed for the MCM4/6/7 (10) and MCM2/4/6/7 (26) complexes purified from HeLa cells. On the other hand, the crystallographic structure of the MthMCM N-terminal portion (residues 2–286) revealed a dodecameric architecture, with two hexameric rings juxtaposed in a head-to-head configuration (27). A remarkable feature of this structure is the presence of a long central channel whose surface has a considerably high positive charge. A three-dimensional reconstruction of the full-sized MthMCM structure by electron microscopy suggests that this central channel runs throughout the entire MthMCM molecule (24). The diameter of the positively charged channel

* This work was supported by European Union Grant QLK3-CT-2002-0207, Ministero dell'Istruzione, Università e Ricerca (MIUR)/Consiglio Nazionale delle Ricerche (Progetto Legge) Grant 449/97-DM 30/10/2000, and MIUR-DM Grant 1105/2002. The costs of publication of this article were defrayed in part by the payment of page charges. This article must therefore be hereby marked "*advertisement*" in accordance with 18 U.S.C. Section 1734 solely to indicate this fact.

¶ To whom correspondence should be addressed. Tel.: 39-081-6132292 (office) or 39-081-6132246 (laboratory); Fax: 39-081-6132277; E-mail: fm.pisani@ibp.cnr.it.

[1] The abbreviations used are: MCM, mini-chromosome maintenance; SsoMCM, *S. solfataricus* MCM; MthMCM, *M. thermoautotrophicum* MCM; Bub-20T, molecule containing a bubble of 20 T residues.

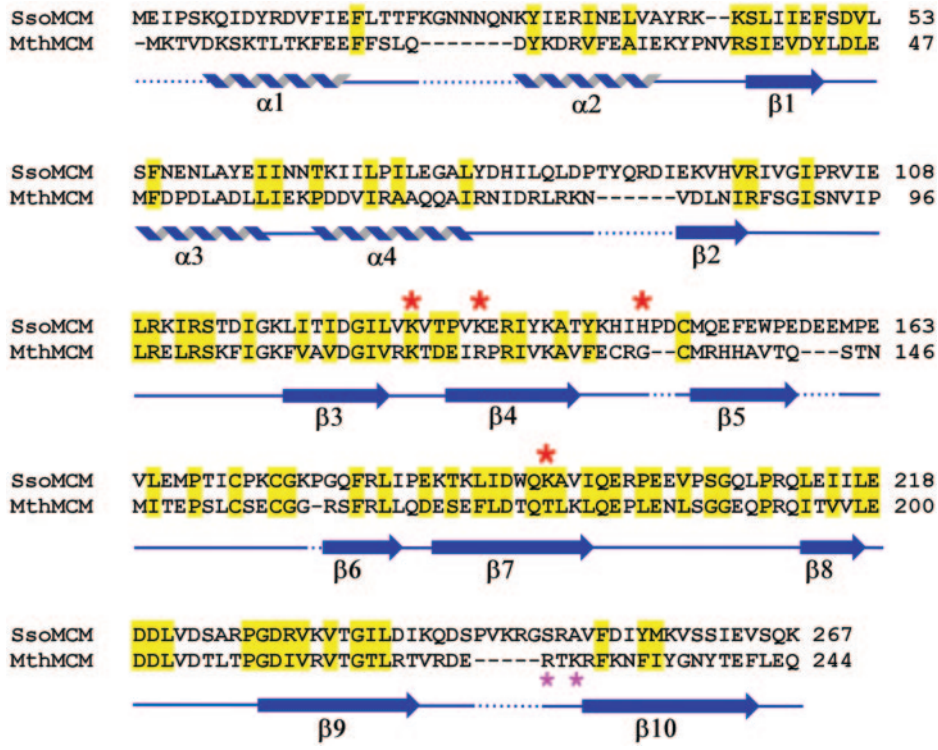

FIG. 1. **Amino acid sequence alignment for the MthMCM and SsoMCM proteins.** The alignment of the MCM proteins from *M. thermoautotrophicum* (MthMCM) and *S. solfataricus* (SsoMCM) was based on a multiple alignment including 12 archaeal enzymes. Highlighted in *yellow* are the amino acids conserved in at least nine of twelve archaeal MCM sequences (the following groups of amino acid residues have been considered similar: Ile/Val/Leu/Met, Phe/Tyr/Trp, Asp/Glu, Ser/Thr, Arg/Lys, and Gly/Ala). The position of the secondary structure elements seen in the structure of the N-terminal domain of the MthMCM protein is shown below the sequence. *Red asterisks* indicate the position of the residues that have been mutated. *Magenta asterisks* indicate the position of the residues that have been shown to affect DNA binding in the MthMCM N-terminal domain (27).

(ranging from 23 to 47 Å) is large enough to accommodate DNA molecules in either single- or double-stranded form (24, 27).

The present study was aimed at identifying amino acid residues of the SsoMCM protein responsible for binding/remodeling DNA. Structure-aided alignment of the MthMCM and SsoMCM sequences revealed four positively charged amino acids (Lys-129, Lys-134, His-146, and Lys-194) of the SsoMCM protein potentially pointing to the center of the putative DNA binding channel. These residues were mutated to alanine, and the site-specific mutants of SsoMCM were purified and characterized. We found that all of the above SsoMCM amino acids participate in DNA binding. Interestingly, the substitution of lysine 134 to alanine was found to affect only binding to duplex molecules, whereas single-stranded DNA binding and helicase activity were not impaired. The results of our analysis have important implications for the understanding of the molecular mechanism of the MCM DNA helicase.

EXPERIMENTAL PROCEDURES

Sequence Alignment—The sequence data base was searched for archaeal homologs of SsoMCM using the BLAST-PSI program (28). Multiple sequence alignments were generated with the ClustalW program (29) and manually modified to account for the positioning of the secondary structure elements in the MthMCM N-terminal domain structure (PDB accession code 1LTL). The sequences comprise MCM proteins from *S. solfataricus* (gene identifier 6015702), *M. thermoautotrophicum* (gene identifier 7428563), *Aeropyrum pernix* (gene identifier 5103579), *Pyrobaculum aerophilum* (gene identifier 18159702), *A. fulgidus* (gene identifier 32485665), *Methanosarcina barkeri* (gene identifier 48840405), *Methanosarcina mazei* (gene identifier 20906360), *Methanosarcina acetivorans* (gene identifier 19917905), *Ferroplasma acidarmanus* (gene identifier 48851904), *Thermoplasma acidophilum* (gene identifier 10640077), *Thermoplasma volcanium* (gene identifier 13541863), and *Picrophilus torridus* (gene identifier 48430937). The following groups of amino acid residues have been considered similar: Ile/Val/Leu/Met, Phe/Tyr/Trp, Asp/Glu, Ser/Thr, Arg/Lys, and Gly/Ala.

Materials—All chemicals were of reagent grade. Restriction and modification enzymes were from New England Biolabs. Radioactive nucleotides were purchased from Amersham Biosciences. Oligonucleotides were synthesized by Proligo (Paris, France).

Plasmids—The *E. coli* expression vector pET19b-SsoMCM was described previously (22). SsoMCM was mutated at lysines 129, 134, and 194 and at histidine 146 to alanine by PCR-based mutagenesis of the corresponding gene (30). The synthetic oligonucleotides used to create the site-directed mutant proteins are available on request. The amplification products were subcloned back into the SsoMCM-pET19b vector and sequenced to check if the desired mutation was present and to rule out that additional mutations were introduced during PCR.

Expression and Purification of Recombinant Proteins—*E. coli* BL21-CodonPlus^{TM}(DE3)-RIL cells (Novagen) transformed with the plasmid expressing the wild type or mutant SsoMCM proteins were grown at 37 °C in 1 liter of Luria-Bertani medium containing 100 μg/ml ampicillin and 100 μg/ml chloramphenicol. When the culture reached an $A_{600\ nm}$ of 0.8 OD, protein expression was induced by the addition of isopropyl-1-thio-β-D-galactopyranoside to 0.2 mM. The bacterial culture was incubated at 37 °C for an additional 2 h. Cells were harvested by centrifugation, and the pellet was stored at −20 °C until use. The pellet was thawed and re-suspended in 10 ml of buffer A (25 mM Tris-HCl, pH 7, and 2.5 mM $MgCl_2$) supplemented with a mixture of protease inhibitors (Sigma). The subsequent steps of the purification procedure were as described previously for the wild type SsoMCM (22).

Gel Filtration Chromatography—Samples of the purified wild type and mutant SsoMCM proteins (100 μg in 250 μl) were subjected to analytical gel filtration chromatography on a Superose 6 HR 10/30 fast protein liquid chromatography column (Amersham Biosciences) equilibrated with 25 mM Tris-HCl, pH 8, 2.5 mM $MgCl_2$, and 100 mM NaCl. The column was run at 0.3 ml/min at room temperature. 0.5-ml fractions were collected and analyzed by Western blot as described previously (22). The column was calibrated by running a set of gel filtration markers that included thyroglobulin (670 kDa), ferritin (440 kDa), and bovine serum albumin (67 kDa).

ATPase Assay—ATPase assay reaction mixture (10 μl) contained 25 mM Hepes-NaOH, pH 7.5, 5 mM $MgCl_2$, 50 mM sodium acetate, 2.5 mM 2-mercaptoethanol, 100 μM [γ-^{32}P]ATP (0.5–1 μCi), and the indicated amounts of protein. Incubations were performed for 30 min at 60 °C in a heated-top PCR machine to prevent evaporation and stopped in ice. A 1-μl aliquot of each mixture was spotted on a polyethyleneimine-cellulose thin layer plate (Merck), pre-run with 1 M formic acid, and developed in 0.5 M LiCl and 1 M formic acid. The amounts of [γ-^{32}P]ATP hydrolyzed to [^{32}P]orthophosphate were quantified using a PhosphorImager (Amersham Biosciences). The amount of spontaneously hydrolyzed ATP was determined using blank reactions without enzyme and subtracted from the reaction rate values calculated as described above.

DNA Substrates—Oligonucleotides were labeled using T4 polynucleotide kinase and [γ-^{32}P]ATP. To prepare the double-stranded sub-

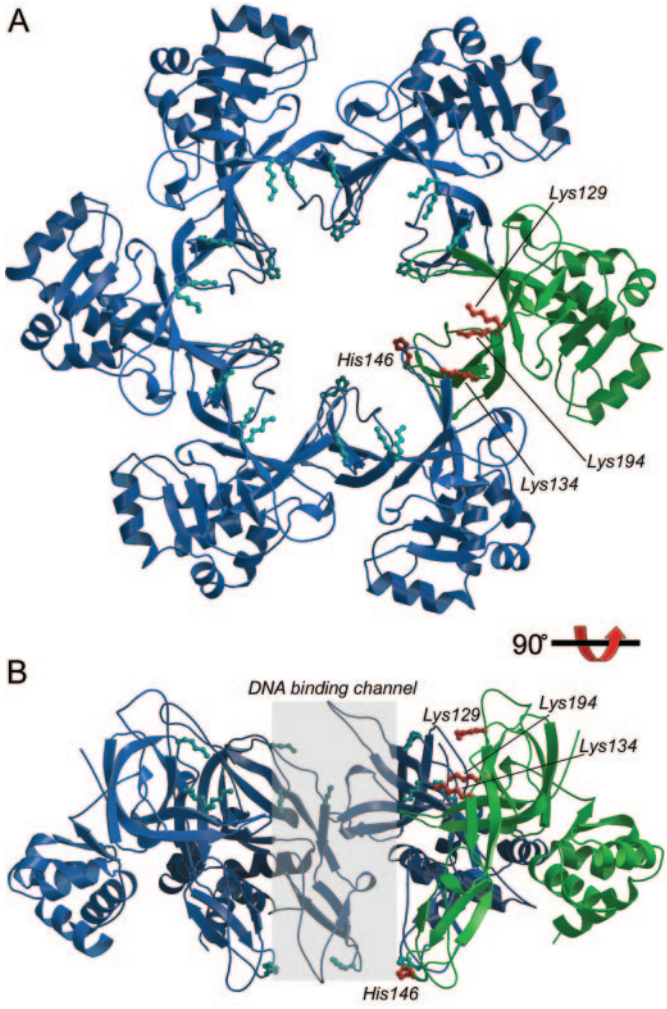

FIG. 2. **Structural location of the residues affecting DNA binding in SsoMCM.** Presented are ribbon representations of an hexamer of the MthMCM N-terminal domain showing the position of the amino acid residues that are the subject of the present study. *A*, the molecule is viewed along the molecular 6-fold axis with one monomer highlighted in *green*. Residues Lys-117, Arg-122, Gly-134, and Thr-176 of the MthMCM structure have been mutated to the corresponding residues in the SsoMCM sequence and are labeled as Lys-129, Lys-134, His-146, and Lys-194 (shown in *red*). The position of the same residues in the other subunits of the hexamer is shown in *light blue*. *B*, the same molecule has been rotated by 90° along a horizontal axis so as to show the 6-fold axis vertical; for the sake of clarity, two monomers have been removed from the front of the molecule to show the inside of the DNA binding channel.

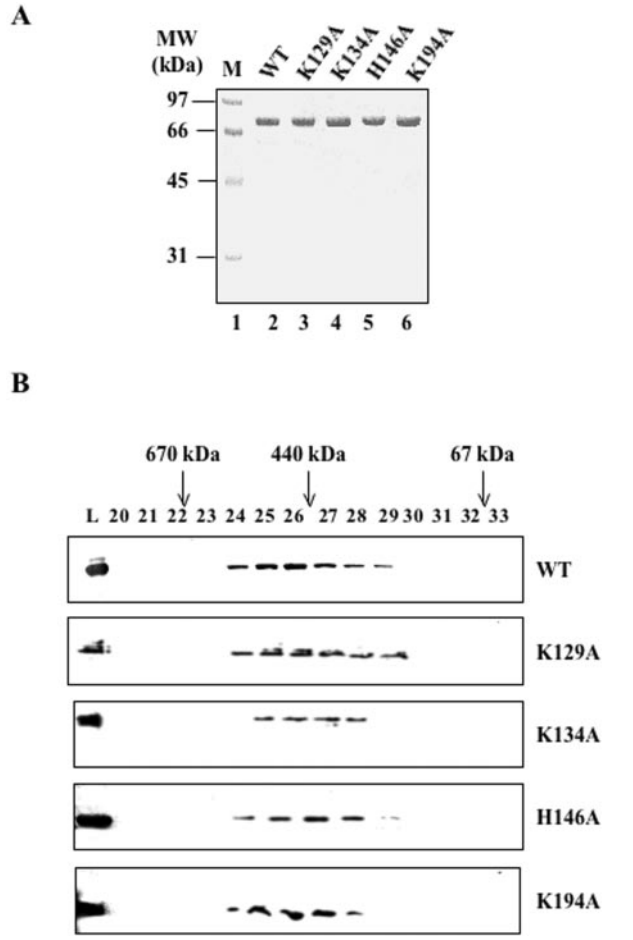

FIG. 3. **The SsoMCM mutants form hexameric complexes.** *A*, aliquots (4 μg) of the purified recombinant proteins used in this study were subjected to 10% SDS-PAGE analysis followed by Coomassie Blue staining. *M* stands for protein size markers. *B*, samples of the purified SsoMCM wild type (*WT*) and mutants (100 μg in 250 μl) were loaded onto a Superose 6 analytical gel filtration column that was run as described under "Experimental Procedures." Aliquots (20 μl) of the indicated fractions were analyzed by Western blot using an anti-SsoMCM antiserum. The peak positions of thyroglobulin (670 kDa), ferritin (440 kDa), and bovine serum albumin (67 kDa) are indicated at the *top* of the panel. *L* stands for load-on.

strates, the labeled oligonucleotide was annealed to a 3-fold molar excess of a cold complementary strand. Substrates containing a bubble made from duplex molecules surrounding poly(dT) (designated Bub-20T) had the sequences 5′-TCTACCTGGACGACCGGG$(T)_{20}$GGGCCAGCAGGTCCATCA-3′ (Bub-20T, top) and 5′-TGATGGACCTGCTGGCCC$(T)_{20}$CCCGGTCGTCCAGGTAGA-3′ (Bub-20T, bottom).

Blunt duplex DNA molecules were constructed by annealing the oligonucleotides 5′-GCTCGGTACCCGGGGATCCTCTAGA-3′ (NoTail-1) and 5′-TCTAGAGGATCCCCGGGTACCGAGC-3′ (NoTail-2). The oligonucleotide Bub-20T-Top was used as the single-stranded DNA substrate.

An 85-mer synthetic oligonucleotide (5′-TTGAACCACCCCCTTGTTAAATCACTTCTACTTGCATGCCTGCAGGTCGACTCTAGAGGATCCCCGGGTACCGAGCTCGAATTCG-3′) was used for the preparation of the DNA helicase substrate. This oligonucleotide is complementary to the M13mp18(+) strand with the exception of a 30-nucleotide 5′-tail (the tail is underlined in the above sequence). The oligonucleotide was labeled with [γ-^{32}P]ATP and T4 polynucleotide kinase, and, after the labeling reaction, it was purified using Quantum Prep PCR Kleen Spin columns (Bio-Rad Laboratories) according to the manufacturer's instructions. To prepare partial duplex DNA molecules, mixtures containing equal molar amounts of each oligonucleotide and the M13mp18(+) strand were incubated for 5 min at 95 °C and then slowly cooled at room temperature.

DNA Band Shift Assays—For each substrate, 10-μl mixtures were prepared that contained 200 fmol of [^{32}P]-labeled DNA in 20 mM Tris-HCl, pH 7.5, 100 mM NaCl, 2 mM EDTA, 0.5 mM $MgCl_2$, 0.7 mM 2-mercaptoethanol, and the indicated amounts of protein. Following incubation for 10–15 min at room temperature, complexes were separated by electrophoresis through 5% polyacrylamide/bis gels (37.5:1) in 0.5× Tris borate-EDTA. Gels were dried down and analyzed by a Storm PhosphorImager using the ImageQuant software (Amersham Biosciences).

DNA Helicase Assay—Helicase assay reaction mixtures (20 μl) contained 25 mM Hepes-NaOH, pH 7.5, 5 mM $MgCl_2$, 50 mM sodium acetate, 2.5 mM 2-mercaptoethanol, 5 mM ATP, and 50 fmol of ^{32}P-labeled substrate (~1×10^3 cpm/fmol). The reactions were incubated for 30 min at 70 °C in a heated top PCR machine to prevent evaporation and stopped by the addition of 5 μl of 5× stop solution (0.5% SDS, 40 mM EDTA, 0.5 mg/ml proteinase K, 20% glycerol, and 0.1% bromphenol blue) and then run on a 8% polyacrylamide-bis gel (29:1) in Tris borate-EDTA containing 0.1% SDS at constant voltage of 150 V. After electrophoresis, the gel was soaked in 20% trichloroacetic acid and analyzed by means of a PhosphorImager (Amersham Biosciences). The reaction products were quantified, and any free oligonucleotide in the absence of enzyme was subtracted.

RESULTS

Four Positive Amino Acid Residues May Be Involved in DNA binding in SsoMCM—The structure of the N-terminal domain of the *M. thermoautotrophicum* MCM (27) provides a useful framework to investigate the structure and function of the MCM homologs. We therefore relied on the MthMCM model to design mutants involved in binding and remodeling DNA in the *S. solfataricus* protein.

Twelve sequences of archaeal MCM proteins were automatically aligned using ClustalW (29), and the alignment was manually modified to take into account the secondary structure information derived from the structure of the MthMCM N-terminal domain. An alignment between the sequences of MthMCM and SsoMCM was extrapolated from the multiple alignment, and the section corresponding to the N-terminal domain is shown in Fig. 1. A very simple homology model was built by threading the sequence of the SsoMCM onto the three-dimensional structure of the MthMCM. No attempt was made to model the insertions or deletions or to energy-minimize the atomic model of the *Sulfolobus* ortholog. The surface of the putative DNA binding channel has been analyzed to look for positively charged residues pointing toward the center and displaying a reasonable level of conservation between archaeal proteins and/or eukaryotic homologs. Four residues have been identified in the SsoMCM sequence that fulfilled these criteria. The position of the residues with respect to the DNA binding channel is shown in Fig. 2.

Lysine 129 (equivalent to Lys-117 in the crystal structure of MthMCM; Fig. 1) is conserved in all the archaeal sequences, with ten sequences possessing a lysine residue and two sequences having an arginine residue. A positively charged residue at this position is also found in the sequences of the eukaryotic MCM3, MCM4, MCM6, and MCM7.

Histidine 146 is located in the turn between strands β4 and β5 at the tip of the zinc finger motif; based on the alignment shown in Fig. 1, it is equivalent to Gly-134 in the structure of MthMCM, but an adjacent two-residue insertion in the SsoMCM sequence will probably make this region assume a slightly different conformation with respect to the existing model. A positively charged residue is present in five of twelve archaeal sequences and in the eukaryotic MCM2 (and some of the MCM3) sequences. Moreover a positive charge pointing toward the channel is also present in the same loop in the MthMCM structure (Arg-133) and has been suggested to be involved in DNA binding (27); this arginine is also found in the MCM5 sequences.

Lysine 194 (equivalent to Thr-176 in the MthMCM structure) is a lysine in all of the archaeal sequences with the sole exception of MthMCM. It is a lysine or an arginine in MCM3, MCM4, MCM6, and MCM7.

The β-hairpin between strands β9 and β10 points directly toward the DNA binding channel in the MthMCM crystal structure. The equivalent loop is longer in *Sulfolobus* and includes four positively charged amino acid residues (Lys-240, Lys-246, Arg-247, and Arg-250). However, we chose not to tackle these residues, because the role of this hairpin in binding DNA has been already established by Fletcher *et al.* in the MthMCM system (27).

The SsoMCM Mutants Exhibit Chromatographic Behavior and ATPase Activity Similar to That of the Wild Type Protein—The SsoMCM gene was mutated at specific sites by a PCR-based method using the pET19b-SsoMCM plasmid (22) as template. The K129A, K134A, H146A, and K194A mutants were overexpressed in *E. coli* cells in soluble form and purified using the same procedure described for the recombinant wild type SsoMCM (Fig. 3*A*). Analytical gel filtration experiments revealed that all of the purified SsoMCM mutants have a hexameric structure with an elution profile similar to the one observed for the wild type protein (Fig. 3*B*).

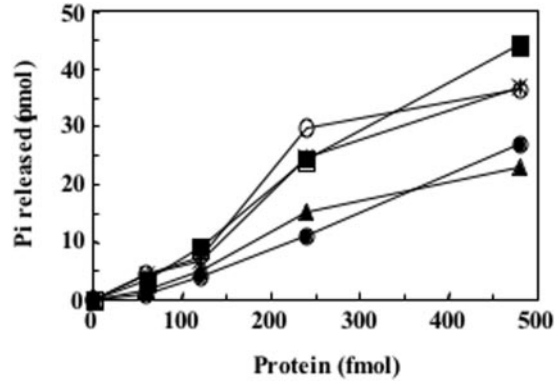

FIG. 4. **The SsoMCM mutants retain full ATPase activity.** ATPase activity assays were carried out with [γ-^{32}P]ATP at 60 °C for 30 min using increasing amounts of wild type SsoMCM and mutants proteins as described under "Experimental Procedures." The orthophosphate released during the hydrolysis reaction was plotted *versus* the amount of protein used in each assay. Results of a typical experiment are reported for each protein. Symbols used are as follows: *filled circle*, wild type; *asterisk*, K129A; *square*, K134A; *triangle*, H146A; *open circle*, K194A.

Because all of the substituted amino acids are located in the N-terminal portion of the SsoMCM polypeptide chain whereas the AAA$^+$ module responsible for the ATP hydrolysis is located in the C-terminal half of the protein, the mutants were expected to retain full ATPase activity. In fact, as shown in Fig. 4, the H146A mutant and the wild type SsoMCM possessed an almost superimposable profile of ATPase activity, whereas the ATP hydrolysis catalyzed by the K129A, K134A, and K194A mutants was found to be even slightly higher than that of the wild type protein. Because the chromatographic behavior, ATPase activity, and oligomeric structure of the SsoMCM mutants appeared to be unchanged with respect to the wild type protein, we argue that the introduced amino acid substitutions have not produced significant perturbations of the overall three-dimensional structure.

DNA Binding Properties of the SsoMCM Mutants—SsoMCM binds DNA with structural specificity displaying a higher affinity for synthetic bubble-containing DNA molecules with respect to blunt duplexes (31). We analyzed the DNA binding ability of the SsoMCM mutants and compared it with that of the wild type protein. DNA band shift assays were carried out with amounts of protein ranging from 160 to 1600 fmol on various DNA ligands, namely molecules containing a bubble of 20 T residues called Bub-20T molecules, blunt duplexes, and single-stranded oligonucleotides as indicated in Fig. 5*A*. Wild type SsoMCM was found to bind the Bub-20T and the single-stranded ligands with higher affinity in regard to the blunt duplexes. However, the bubble-containing DNA molecules were preferred by SsoMCM over the single-stranded oligonucleotides. Analysis of the binding properties of the site-specific mutants revealed that the substitution of Lys-129, Lys-194, or His-146 with alanine completely abolished the DNA binding ability on all of the tested ligands (see Fig. 5, *B–D*). In contrast, the K134A mutant was able to bind single-stranded DNA with an affinity comparable with that of the wild type SsoMCM (see Fig. 5, *A* and *B*), and its ability to bind the Bub-20T ligand was only slightly reduced (see Fig. 5, *A–D*), whereas it was almost completely unable to bind blunt duplex molecules (see Fig. 5, *A–C*). These results indicated that the SsoMCM residues Lys-129, Lys-134, and Lys-194 are critical for binding DNA in either single- or double-stranded form, whereas Lys-134 seems

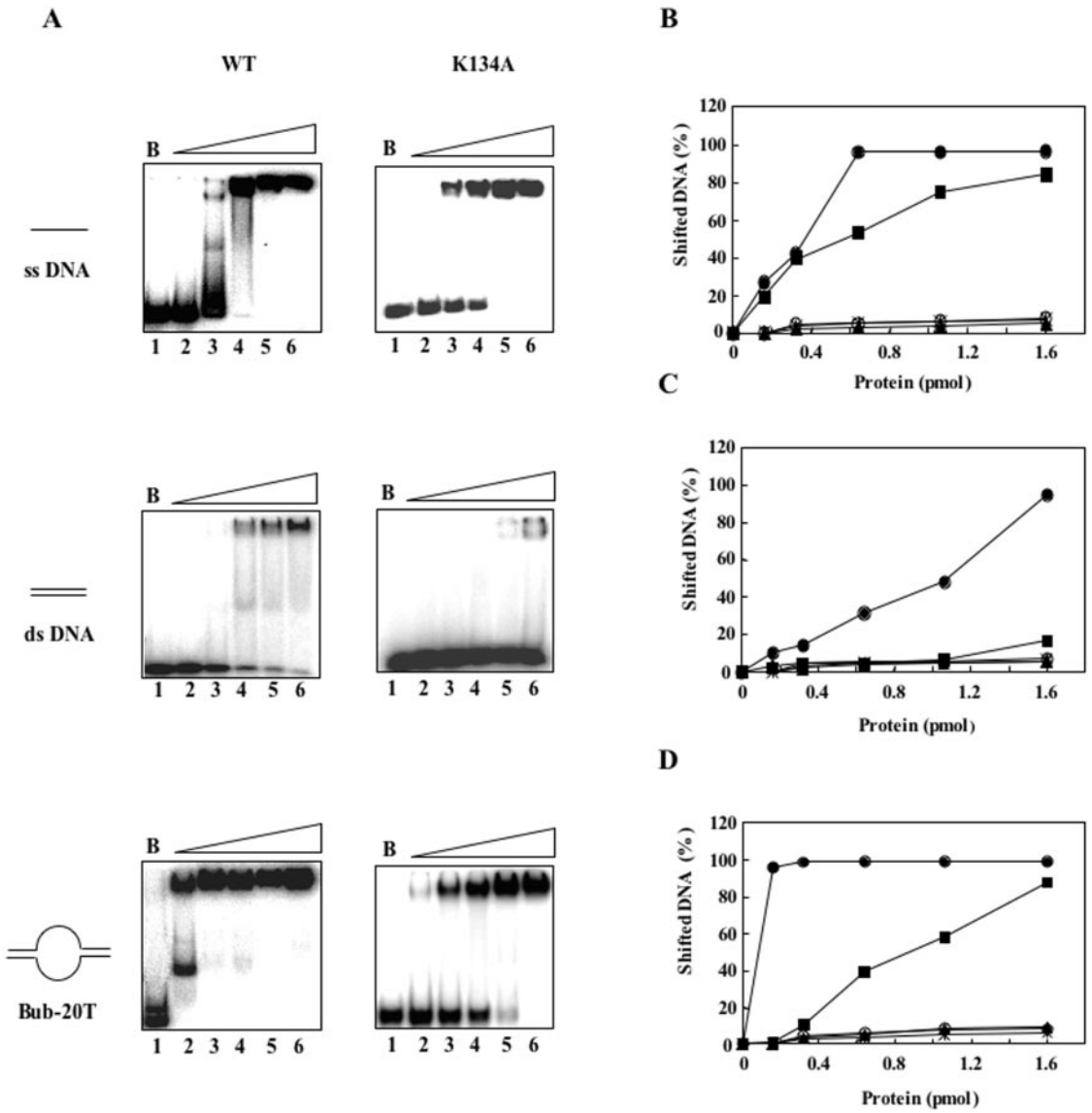

FIG. 5. **DNA binding properties of wild type SsoMCM and mutants proteins.** *A*, DNA band-shift assays were carried out using the DNA molecules schematically depicted and increasing amounts of wild type (*WT*) SsoMCM and the K134A mutant (75, 150, 300, 500, and 750 ng of protein in *lanes 2–6*, respectively, of each gel) as described under "Experimental Procedures." The lanes marked with *B* (*lane 1* of each gel) were loaded with control samples without protein. *ss*, single-stranded; *ds*, double stranded. Plots of the shifted DNA *versus* the amount of protein are shown. Single-stranded DNA (*B*), blunt duplex (*C*), and Bub-20T ligand (*D*) were used as ligands in these assays. Results of a typical experiment are reported for each protein. Symbols used are as described in the legend to Fig. 4.

to be mainly involved in the interaction with the double-stranded DNA molecules.

The SsoMCM K134A Mutant Retains Full DNA Helicase Activity—Next, we tested the strand-displacement capability of the SsoMCM site-directed mutants alongside that of the wild type protein. As reported previously, SsoMCM displayed a low level of helicase activity on substrates made of oligonucleotides fully annealed to single-stranded M13 DNA, whereas the presence of a 9- or a 30-nucleotide tail on the 5′-end of the oligomer was found to markedly stimulate the unwinding activity of the enzyme (22). Therefore, we used DNA duplexes that contained a 30-nucleotide 5′-tail as the substrate for the DNA helicase assays. As expected,, the K129A, H146A, and K194A mutants were found to be completely unable to unwind this DNA substrate even when ~2 pmol of hexameric protein were present in the assay mixture. On the other hand, the DNA helicase activity of the K134A mutant was not impaired with respect to the wild type protein, as shown in Fig. 6, *A* and *B*. Because the amino acid Lys-134 was found to be critical for the interaction with DNA molecules in the double- but not in the single-stranded form, the finding that its substitution does not affect the DNA helicase activity suggests that the ability of the enzyme to bind single- but not double-stranded DNA is required for the unwinding function.

DISCUSSION

The three-dimensional structure of the MthMCM protein revealed a dodecameric assembly made of two ring-like hexamers with a long central channel highly positively charged. The shape and electrostatic character of the channel strongly suggests that its role is to bind DNA; however its size is much wider than the channels seen in other helicases whose structures are known and is therefore large enough to bind both single- or double-stranded DNA (27). The channel is constricted in the middle by six β-hairpin "fingers" pointing toward the center and closely linked with the ATPase domain. These fingers are formed by the strands β9 and β10 and contain several arginine/lysine residues that are likely to participate in the

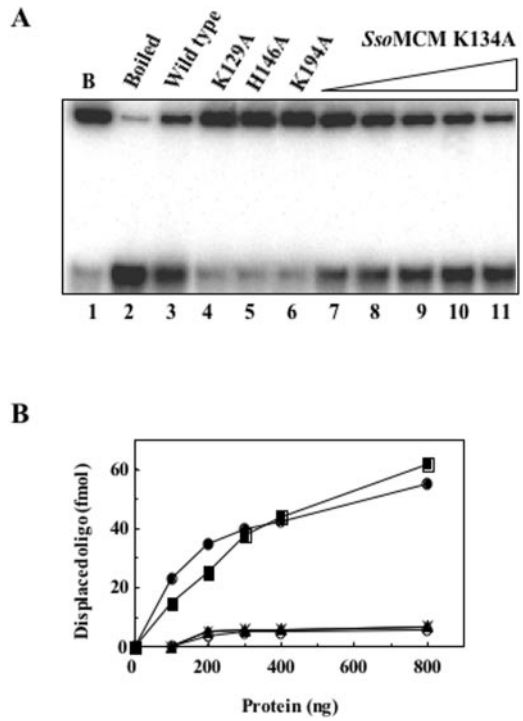

FIG. 6. **DNA helicase activity of SsoMCM wild type and mutant proteins.** DNA helicase activity assays were carried out using DNA duplexes made of a 30-nucleotide 5′-tailed oligonucleotide annealed to single-stranded M13 DNA as described under "Experimental Procedures." *A*, DNA unwinding assays were performed using the SsoMCM wild type, the K129A, H146A, and K194A mutants (800 ng; *lanes 3–6*), and increasing amounts of the K134A mutant (100, 200, 300, 400, 800 ng, *lanes 7–11*, respectively). Lanes marked with *B* (*lane 1*) and *Boiled* (*lane 2*) were loaded with assay mixtures without protein that were incubated at 70 °C or boiled, respectively. *B*, the oligonucleotide displaced by wild type SsoMCM and the mutant proteins was quantified by phosphorimaging and plotted *versus* the amount of protein used in each activity assay. Results of typical experiments are reported for each protein. Symbols used are as described in the legend to Fig. 4.

interaction with the nucleic acids. Mutation of two positively charged residues located on the tip of the hairpins in MthMCM (Arg-226 and Arg-228) abolishes binding to both single- and double-stranded DNA. Thus, it was proposed that the ATP hydrolysis-driven shifting of the six fingers may supply a mechanism by which DNA is remodeled and translocated through the central channel during the helicase function (27).

Structure-guided multiple sequence alignments suggest that the fold of the MthMCM protein N-terminal portion is conserved among the archaeal and eukaryal MCM homologs despite the lower degree of conservation of their primary structures. This hypothesis is supported by the finding that a number of basic charged residues located on the channel surface of the MthMCM are conserved in the MCM proteins (27). In this study we investigated the functional role of some of these conserved amino acids by site-specific mutagenesis of the SsoMCM protein. We decided to exclude from our analysis the conserved arginine/lysine residues located in the β-hairpin fingers, because their involvement in DNA binding has been already established for the MthMCM (27). As targets for our site-directed mutagenesis studies, we selected amino acids of the SsoMCM N-terminal portion that are positively charged, conserved among archaeal and eukaryal MCM proteins, exposed on the surface of the putative DNA binding channel, and not involved in intra- or inter-molecular contacts as suggested by multiple sequence alignments and inspection of the MthMCM crystallographic structure. The four identified residues (Lys-129, Lys-134, His-146, and Lys-194) were shown to be truly involved in the interaction with DNA because their substitution with alanine residues impaired the ability of SsoMCM to bind nucleic acids. The present study provides the first experimental evidence that the above residues play a direct role in the DNA binding/remodeling function in an MCM complex. Our results provide additional support to the hypothesis that the MthMCM central channel encircles DNA and plays a critical role in the unwinding function.

The molecular mechanism of the MCM helicase action has not yet been clarified, and three models have been proposed to date. In one model, during helicase action the MCM complex encircles only one strand of the duplex (corresponding to the leading strand of a replication fork) and pulls it in the 3′ to 5′ direction, whereas interaction with the other strand is not required (32). Unwinding of the DNA helix is therefore caused by the steric exclusion of the other strand. This mechanism is similar to the one proposed for the bacterial and phage replicative helicases, although these enzymes unwind DNA with 5′ to 3′ polarity, binding the lagging strand of the replication fork (33–35). In contrast, the two other models both predict that during the unwinding reaction the MCM complex encircles DNA in double-stranded form. In the "rotary pump" mechanism, multiple MCM rings actively translocate along duplex DNA, twist it, and produce a physical separation of the two strands at a distance (36). This model is reminiscent of the one proposed for RuvB, an AAA^+ protein that is involved in Holliday junction remodeling (37). The third mechanism is based on an analysis of the crystallographic structure of the large T antigen helicase of the simian virus SV40 (38). This hexameric ring-shaped molecule possesses a large positively charged central "chamber" with "holes" on the side walls. In the proposed mechanism, two hexamers arranged in a head-to-head configuration bind the viral replication origin sequence and pump double-stranded DNA into the central chamber, whereas the melted strands are extruded through the lateral holes. Because both the central DNA-binding channel and the lateral holes seem to be present also in the MthMCM, it was hypothesized that these two ring-like helicases possess a similar mechanism of action (24, 27, 38).

It is worth trying to analyze the behavior of the SsoMCM K134A mutant described in this study in the contest of the three proposed models. We found that the substitution of lysine 134 with alanine in SsoMCM affects only binding to double-stranded DNA, whereas the single-stranded DNA binding function and the DNA helicase activity are not impaired. Therefore, the ability of SsoMCM to bind duplex molecules does not seem to be required for the DNA unwinding. This result is consistent with the DnaB-like mechanism of DNA helicase action predicting that the ring-like complex encircles only one strand. This model is also supported by our finding that the SsoMCM helicase activity is greatly enhanced on forked DNA molecules, whereas it is almost completely inactive on duplexes without a 5′-tail (22). A similar behavior was also observed for the MCM4/6/7 complex of *S. pombe* (9), *S. cerevisiae* (32), and *H. sapiens* (39).

In addition, in the present study we found that SsoMCM binds single-stranded and fork-containing DNA molecules with higher affinity than blunt duplexes, as detected by band shift assays. It was recently demonstrated that MthMCM and the MCM4/6/7 complex of *S. pombe* and *S. cerevisiae* are able to encircle duplex DNA molecules and actively translocate along them (20, 32). This capability might enable the MCM complex to accomplish additional tasks *in vivo* such as driving DNA branch migration during DNA repair/recombination reactions. Additional studies are required to unravel the mechanisms of hexameric DNA helicase action. Our biochemical analysis in-

dicates that investigating the molecular determinants of the SsoMCM helicase function may provide useful hints for understanding how the more complex eukaryotic MCM proteins bind and remodel DNA.

REFERENCES

1. Tye, B. K. (1999) *Annu. Rev. Biochem.* **68,** 649–686
2. Forsburg, S. L. (2004) *Microbiol. Mol. Biol. Rev.* **68,** 109–131
3. Neuwald, A. F., Aravind, L., Spouge, J. L., and Koonin, E. V. (1999) *Genome Res.* **9,** 27–43
4. Labib, K., Tercero, J. A., and Diffley, J. F. (2000) *Science* **288,** 1643–1647
5. Thömmes, P., Kubota, Y, Takisawa, H., and Blow, J. J. (1997) *EMBO J.* **16,** 3312–3319
6. You, Z., Komamura, Y., and Ishimi, Y. (1999) *Mol. Cell. Biol.* **19,** 8003–8015
7. Lee, J. K., and Hurwitz, J. (2000) *J. Biol. Chem.* **275,** 18871–18878
8. Ishimi, Y. (1997) *J. Biol. Chem.* **272,** 24508–24513
9. Lee, J.-K., and Hurwitz, J. (2001) *Proc. Natl. Acad. Sci. U. S. A.* **98,** 54–59
10. Sato, M., Gotow, T., You, Z., Komamura-Kohno, Y., Uchiyama, Y., Yabuta, N., Nojima, H., and Ishimi, Y. (2000) *J. Mol. Biol.* **300,** 421–431
11. Ishimi, Y., Komamura, Y., You, Z., and Kimura, H. (1998) *J. Biol. Chem.* **273,** 8369–8375
12. Schwacha, A., and Bell, S. P. (2001) *Mol. Cell* **8,** 1093–1104
13. Davey, M. J., Indiani, C., and O'Donnell, M. (2003) *J. Biol. Chem.* **278,** 4491–4498
14. Kelman, L. M., and Kelman, Z. (2003) *Mol. Microbiol.* **48,** 605–615
15. Grabowski, B., and Kelman, Z. (2003) *Annu. Rev. Biochem.* **57,** 487–516
16. Kelman, Z., Lee, J.-K., and Hurwitz, J. (1999) *Proc. Natl. Acad. Sci. U. S. A.* **96,** 14783–14788
17. Chong, J. P. J., Hayashi, M. K., Simon, M. N., Xu, R.-M., and Stillman, B. (2000) *Proc. Natl. Acad. Sci. U. S. A.* **97,** 1530–1535
18. Shechter, D. F., Ying, C. Y., and Gautier, J. (2000) *J. Biol. Chem.* **275,** 15049–15059
19. Poplawski, A., Grabowski, B., Long, S. E., and Kelman, Z. (2001) *J. Biol. Chem.* **276,** 49371–49377
20. Shin, J.-H., Jiang, Y., Grabowski, B., Hurwitz, J., and Kelman, Z. (2003) *J. Biol. Chem.* **278,** 49053–49062
21. Kasiviswanathan, R., Shin, J.-H., Melamud, E., and Kelman, Z. (2004) *J. Biol. Chem.* **279,** 28358–28366
22. Carpentieri, F, De Felice, M., De Falco, M., Rossi, M., and Pisani, F. M. (2002) *J. Biol. Chem.* **277,** 12118–12127
23. Grainge, I., Scaife, S., and Wigley, D. B. (2003) *Nucleic Acids Res.* **31,** 4888–4898
24. Pape, T., Meka, H., Chen, S., Vicentini, G., van Heel, M., and Onesti, S. (2003) *EMBO Rep.* **4,** 1079–1083
25. Yu, X., VanLoock, M. S., Poplawski, A., Kelman, Z., Xiang, T., Tye, B. K., and Egelman, E. H. (2002) *EMBO Rep.* **3,** 792–797
26. Yabuta, N., Kajimura, N., Mayanagi, K., Sato, M., Gotow, T., Uchiyama, Y., Ishimi, Y., and Nojima, H. (2003) *Genes Cells* **8,** 413–421
27. Fletcher, R. J., Bishop, B. E., Leon, R. P., Sclafani, R. A., Ogata, C. M., and Chen, X. S. (2003) *Nat. Struct. Biol.* **10,** 160–167
28. Altschul, S. F., Gish, W., Miller, W., Myers, E. W., and Lipman, D. J. (1990) *J. Mol. Biol.* **215,** 403–410
29. Thompson, J. D., Gibson, T. J., Plewniak, F., Jeanmougin, F., and Higgins, D. G. (1997) *Nucleic Acids Res.* **25,** 4867–4882
30. Ho, S. N., Hunt, D. H., Horton, R. M., Pullen, J. K., and Pease, L. R. (1989) *Gene* **77,** 51–59
31. De Felice, M., Esposito, L., Pucci, B., De Falco, M., Rossi, M., and Pisani, F. M. (2004) *J. Biol. Chem.* **279,** 43008–43012
32. Kaplan, D. L., Davey, M., and O'Donnell, M. (2003) *J. Biol. Chem.* **278,** 49171–49182
33. Hacker, K. J., and Johnson, K. A. (1997) *Biochemistry* **36,** 14080–14087
34. Ahnert, P., and Patel, S. S. (1997) *J. Biol. Chem.* **272,** 32267–32273
35. Kaplan, D. L. (2000) *J. Mol. Biol.* **301,** 285–299
36. Laskey, R. A., and Madine, M. A. (2003) *EMBO Rep.* **4,** 26–30
37. Putnam, C. D., Clancy, S. B., Tsuruta, H., Gonzalez, S., Wetmur, J. G., and Tainer, J. A. (2001) *J. Mol. Biol.* **311,** 297–310
38. Li, D., Zhao, R., Lilyestrom, W., Gai, D., Zhang, R., DeCaprio, J. A., Fanning E., Jochimiak, A., Szakonyl, G., and Chen, X. S. (2003) *Nature* **423,** 512–518
39. You, Z., Ishimi, Y., Mizuno, T., Sugasawa, K., Hanaoka, F., and Masai, H. (2003) *EMBO J.* **22,** 6148–6160

Amino Acids of the *Sulfolobus solfataricus* Mini-chromosome Maintenance-like DNA Helicase Involved in DNA Binding/Remodeling

Biagio Pucci, Mariarita De Felice, Mosè Rossi, Silvia Onesti and Francesca M. Pisani

J. Biol. Chem. 2004, 279:49222-49228.
doi: 10.1074/jbc.M408967200 originally published online September 14, 2004
